Microfluidics and Nanofluidics (2018) 22:94
https://doi.org/10.1007/s10404-018-2112-y

RESEARCH PAPER

A positive pressure-driven PDMS pump for fluid handling in microfluidic chips

Bendong Liu[1] · Mohan Li[1] · Baohua Tian[1] · Xu Yang[1] · Jiahui Yang[1]

Received: 17 May 2018 / Accepted: 3 August 2018 / Published online: 18 August 2018

Abstract
By utilizing the high gas permeability of polydimethylsiloxane (PDMS), a simple positive pressure-driven pumping method was introduced. The pump was an aerated PDMS with a central channel in it and packing with a transfusion bottle. It could be attached to the inlet of microfluidic chip using a Teflon tube to release the air into the microfluidic system and then to create a positive pressure for driving fluid. In comparison with the degas-based PDMS pump, positive pressure-driven PDMS pump offered increased system flexibility and reduced individual device fabrication complexity due to its independence and versatility. More importantly, it offered the advantages that the PDMS pump could be wrapped in transfusion bottles to meet the readily available requirements, and it also easily assembled, which only required the user use a Teflon tube to connect a PDMS pump and a microfluidic chip. This assembly provided great freedom to meet different pumping requirements. Furthermore, this PDMS pump could offer many possible configures of pumping power by adjusting the geometries of the pump or by combining different pump modules, the adjustment of pumping capacity was investigated. To help design pumps with a suitable pumping performance, the sealing effect, pumping pressure and flow rate were also investigated. The results indicated that the performance of the positive pressure-driven PDMS pump was reliable. Finally, we demonstrated the utility of this pumping method by applying it to a PDMS-based viscometer microfluidic chip.

Keywords Positive pressure · Gas solubility · Gas permeability · PDMS pump · Microfluidics

1 Introduction

As an emerging technology, microfluidics are widely used in the fields of biochemical analysis (Mojica et al. 2016; Xu et al. 2015), biomedical engineering (Bourbaba et al. 2016; Pandele et al. 2017) and environmental monitoring (Das 2016). Microfluidic devices have numerous advantages including reducing the reagent consumption, improving the analysis speed, have high precision and reliability, and portability. The usefulness of a microfluidic system lies in its ability to integrate different components such as actuators, mixers, valves, pumps, etc., which eventually lead to the development of micro total analysis systems (μTAS), commonly known as lab-on-a-chip (Manz et al. 1990). Currently, traditional pumps such as syringe pumps, peristaltic pumps, and regulated source of pressure or vacuum are widely used in microfluidic systems. These pumps make a precise and reliable control of the fluid flow in microchannels, but the portability is limited due to their size (Iverson and Garimella 2008). To increase the device portability, numerous research efforts have been made by utilizing piezoelectric (Opekar et al. 2016; He et al. 2017), electrostatic (Sheikhlou et al. 2015) or magnetic effects (Barker et al. 2016) but meanwhile these pumps increase the cost.

A more practical pumping method for portable microfluidic systems that requires neither any external power nor expensive on-chip microfluidic components has been proposed by Hosokawa et al. (2004). This negative pressure-driven pumping mechanism takes advantage of the inherent porosity and air solubility of PDMS. By vacuuming air from the bulk PDMS, a pressure difference associated to atmospheric pressure is created. After a sample is loaded into closed microchannels, this pressure difference which generates negative pressure causes air inside the microchannels to diffuse into the bulk PDMS and pulls the fluids from inlets into the microfluidic chip. Thus, devices that utilize

✉ Bendong Liu
liubendong@bjut.edu.cn

[1] College of Mechanical Engineering and Applied Electronics Technology, Beijing University of Technology, Beijing 100124, China

this phenomenon are capable of running without any external power. This power-free pumping has previously been demonstrated for microchip immunoassays (Garg et al. 2016), gold nanoparticle-based DNA analysis (Hasegawa et al. 2015), and cell loading (Luo et al. 2010).

However, the pumping capacity of this type of pump is relatively fixed for a given PDMS microfluidic chip, and the working time is also short as the air distribution inside and outside the PDMS reaches the equilibrium soon after the degassed PDMS microchip is placed in atmosphere. More unfavorably, this pump is only compatible with a given PDMS microfluidic chip, which greatly limits its application scope in microfluidic systems.

To address the above limitations, we have developed a positive pressure-driven PDMS pump for portable microfluidic applications. In comparison with the degas-based PDMS pump to microfluidic systems, positive pressure-driven PDMS pump offers increased system flexibility and reduced individual device fabrication complexity due to its independence and versatility. More importantly, it offers the advantages that the PDMS pump can be wrapped in transfusion bottle to meet the readily available requirements, and it also easily assembled, which only requires the user use a Teflon tube to connect a PDMS pump and a microchip. Furthermore, this PDMS pump can offer many possible configures of pumping power by adjusting the geometries of the pump or by combining different pump modules. Our design makes the PDMS pump as an independent module and solves the problem of low pumping capacity of degas-based PDMS pump, but both the degas-based PDMS pump and positive pressure-driven PDMS pump can only be used as infusion-only pump and the pump cannot be stopped after being started are still waiting for further research.

2 Theory

As shown in Fig. 1, positive pressure-driven PDMS pump is a small transfusion bottle which is filled with PDMS and have a channel in the central of it. First, the pump is placed in the gasholder and then connected to the air compressor through a Teflon tube. By opening the air compressor, high pressure will be generated inside the gasholder. The pressure difference between the gasholder and pump allows air diffusion into the PDMS pump. After a period of time, the pump can be pulled out of the gasholder and then release gas into the air due to pressure difference. Therefore, the fluid can be driven inside the Teflon tube which inserted into the central channel of the pump. This approach facilitates a straight forward positive pressure pumping system that can be used with many microfluidic systems.

The working mechanism of the positive pressure-driven PDMS pump is based on the release of air in a closed system from PDMS. First, the air diffusion into PDMS in the gasholder and then the air release from PDMS when the pump is working. The process of air diffusion into PDMS can be characterized as a solution-diffusion process (George and Thomas 2001). Air solution first occurs at the surface of the PDMS and then dissolved air molecules diffuse into the interior of the PDMS. The solution process can be described in Henry's law (Miller and Vandome 2010), and the Henry's law shows that the equilibrium concentration of air dissolved in PDMS

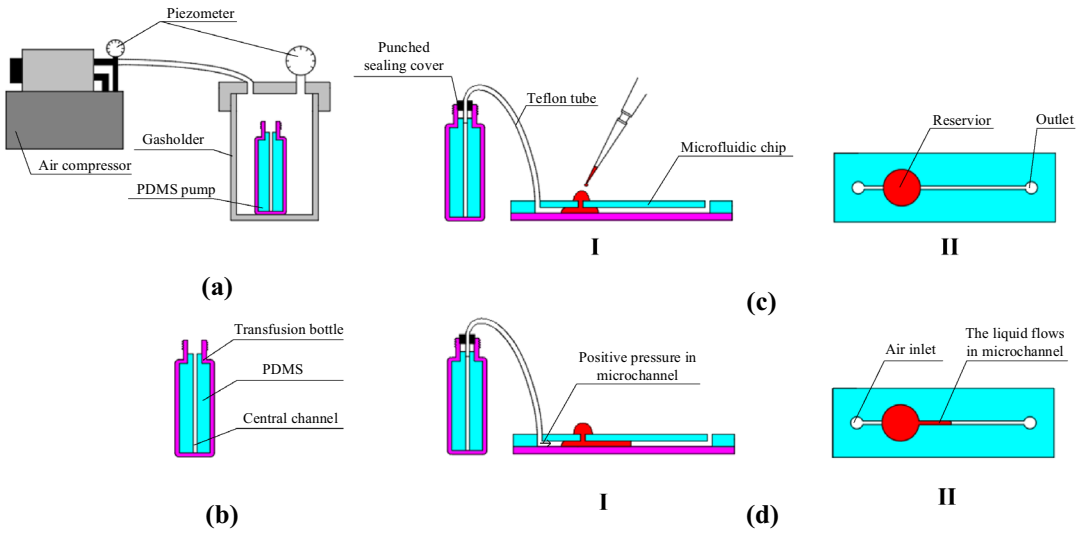

Fig. 1 Schematic illustration of the operation of the positive pressure-driven PDMS pump. **a** The aerating of the PDMS pump. **b** The composition of the PDMS pump. **c** The formation of the closed microfluidic system after a droplet of liquid was loaded into the inlet. **d** The liquid was driven into the microchannel under the positive pressure which created by the PDMS pump

is directly proportional to the partial pressure of the air around the PDMS as

$$C = S \cdot P \tag{1}$$

where C is the concentration of air molecules in PDMS, S is the solubility coefficient of air in PDMS, and P is the pressure of air.

When a PDMS pump is placed in a gasholder which provide a high-pressure environment, the air dissolved into PDMS owing to its high solubility and a high-pressure dissolution equilibrium is established. After it is brought back to the atmosphere, the original equilibrium is broken, and air release to the atmosphere until a new equilibrium is reached (Li et al. 2012). In terms of solubility, the amount of air transported into PDMS, Δm, can be written as

$$\Delta m = (C_0 - C_{\text{atm}})V_{\text{PDMS}} = S(P_0 - P_{\text{atm}})V_{\text{PDMS}} \tag{2}$$

where C_0 and C_{atm} are the equilibrium concentrations of air in PDMS at high-pressure environment and atmosphere; respectively, P_0 and P_{atm} are the air pressure around PDMS at high-pressure environment and atmosphere, respectively; and V_{PDMS} is the volume of the PDMS inside the pump. This equation indicates that the amount of air transferred into PDMS depends on both the size of the PDMS and the high-pressure environment level.

For the steady-state flux across PDMS, the flow rate can be determined by Skelley and Voldman (2008)

$$Q = \frac{PA(P_0 - P_{\text{atm}})}{\text{t}} \frac{T}{273} \frac{76}{P_{\text{atm}}} \tag{3}$$

where Q is the volumetric flow rate, A is the diffusion area, T is the absolute temperature in kelvin and P_{atm} is the atmospheric pressure. For this model, it is assumed that the steady-state flux will be significantly larger across the PDMS than any flux into the bulk PDMS and the pumping time can also be calculated by this.

From Eqs. (2) and (3), the Δm and Q are directly proportional to the pressure difference ($\Delta P = P_0 - P_{\text{atm}}$). The maximum pressure difference ($\Delta P = P_{\text{atm}} - P_0$) of negative pressure pumping method can be considered as 1 atm, since the meaning of absolute vacuum is that the gas pressure is zero in a given space, and it can never be achieved (Smetana and Carley 1966). The pressure difference of this positive pressure-driven PDMS pump in this paper can be reached 4 atm. For high-pressure air compressors, pressure difference can even become larger. Accordingly, the driving capability of positive pressure driving can be several times than the negative pressure driving.

When the PDMS pump is working, the rough estimate of the characteristic time to allow for the air across the PDMS can be obtained by examining the diffusion time t across the PDMS (Xu et al. 2014):

$$t \approx w^2 D^{-1} \tag{4}$$

where w is the thickness of the PDMS and D is the diffusion coefficient of air in PDMS.

The air release from the PDMS pump causes the liquid flow in the micro-channel. If we assume that the air concentration or the air density inside the channel is unchanged during the pumping process, the volumetric flow rate Q and the pumped fluid volume V inside the channel can be expressed as (Xu et al. 2014):

$$Q(t) \approx k\frac{FS(t)}{C_{\text{ATM}}} = kD\frac{C_{\text{PDMS}} - C_{\text{Chamber}}}{C_{\text{ATM}}}\frac{S(t)}{w} \Rightarrow V(t) = \int Q(t)\mathrm{d}t \tag{5}$$

where k is an empirical factor decided by viscous effect of the pumped liquid flow and $S(t)$ is the exchange surface area that allows air release from the PDMS pump. Equation (5) points out that there are two major parameters that can affect the flow rate: the thickness of the PDMS pump (w) and the exchange surface area (S) that allows air release from the PDMS pump.

3 Experimental section

3.1 Design and fabrication of PDMS pump

The proposed PDMS pump was a small transfusion bottle (Fig. 1b) which filled with PDMS and a channel in the central of it. The Teflon tube (Hefei Haicheng Industrial Technology Co. Ltd, China) connected the PDMS pump and the microfluidic chip so that the PDMS pump could drive the liquids in the microfluidic chip. The central channel was designed to adjust the diffusion area by changing the position of the Teflon tube in the channel.

The fabrication of PDMS pump was done in the super clean room. First, the transfusion bottle (Xuzhou Ming Zheng glass products Co. Ltd, China) was cleaned using acetone and methanol, respectively, and then rinsed in deionized water before blown dry by filtered nitrogen gas. After cleaning, the cleaned transfusion bottle was placed on a hot plate at 90 °C for 20 min to make it completely dried. Then, the prepolymer of PDMS (Sylgard 184, Dow Corning) and corresponding curing agent was thoroughly mixed at a ratio of 10:1 (wt/wt). And the mixed PDMS was degassed in a vacuum chamber for 40 min to remove all the air bubbles. After that, the PDMS mixture was carefully poured into the transfusion bottle with a core module lied in the center of the bottle and then baked on a hot plate at 90 °C for 2 h. Finally, the core module was removed from PDMS.

3.2 Operation of PDMS pump

A basic operational schematic for the PDMS pump is shown in Fig. 1. To activate the PDMS pump, the pump was placed

in a gasholder and then connected to the air compressor and pumped at 50 kPa for 24 h (Fig. 1a). Subsequently, the PDMS pump was taken out from the gasholder and connected directly into the inlet of a microfluidic chip with a Teflon tube (Fig. 1c). To reduce gas leakage, the sealing cover was punched which the Teflon tube goes through. After that, liquid samples were loaded onto the inlets using a conventional micropipette (Fig. 1c). Under the positive pressure created by the PDMS pump, the samples were pushed into the microchip (Fig. 1d).

3.3 Adjustment of pumping capacity

The pumping capacity can be roughly adjusted by central channel, which is designed to adjust the diffusion area by changing the position of Teflon tube in the channel. In this experiment, three kinds of adjustment mode were designed. The Teflon tubes were inserted into the center channel at 5, 10, 15 mm from the bottom (Fig. 2a–c), thus, the height of the diffusion area was 5,10,15 mm, respectively. The experimental setup for adjusting pumping capacity of positive pressure-driven PDMS pump is shown in Fig. 2d. The pumping capacity of different adjustment modes were evaluated by monitoring the working time and height of elevation of the liquid column in the tube. A vertically positioned variable diameter Teflon tube with one end connected to the central channel of PDMS pump was used for measuring the pumping capacity. The tube was 1000 μm in inner diameter and 100 cm in length. Dye solution was served as the pumping liquid for direct optical visibility. During the measurement, a positive-driven PDMS pump which was taken from the gasholder at 50 KPa for 24 h was adhered to the surface of the elevator, and then, the tube was inserted into the central channel of the pump. The variable diameter of the tube was filled with dye solution. For all experiments, the idle time was 2 min, which was defined as the PDMS pump exposed to atmospheric conditions before sample liquid blocks the inlets of the tube or the microfluidic chips equipped with the PDMS pump.

3.4 Characterization of PDMS pump

The most important and basic parameters related to the positive pressure-driven PDMS pump are back pressure and flow rate; therefore, measurements of back pressure and flow rate were done in this study. To compare the positive and the negative pressure-driving capacity, back pressure and flow rate of the negative pressure-driven pump were also tested. The test environment and conditions were the same with positive pressure-driven PDMS pump, and experimental setups were also similar to the positive pressure-driven PDMS pump. The PDMS pump which the Teflon tube inserted into the center channel 15 mm from the bottom is used in this experiment.

In this experiment, there are three factors to the back pressure (P): static fluid pressure (P_s), capillary pressure (P_c), and dynamic pressure (P_d); and $P = P_s + P_c + P_d$. P_s is the pressure contributed by the potential energy of the fluid in the tube, i.e., $P_s = \rho g h$, where g is the acceleration of gravity, and h is the height of the liquid column in the tube. P_c is the pressure contributed by capillary force, which is about 70 Pa according to the calculation of Li et al. (2012). P_c is affected by the dynamic contact angle which is about 110° between pure water and Teflon (Goswami et al. 2008). The contact angle will be decreased when the theoretical capillary pressure is reduced. As a result, the P_c of Teflon tube is negligible. P_d is the pressure contributed by the kinetic energy of the fluid in the tube which is affected by the flow

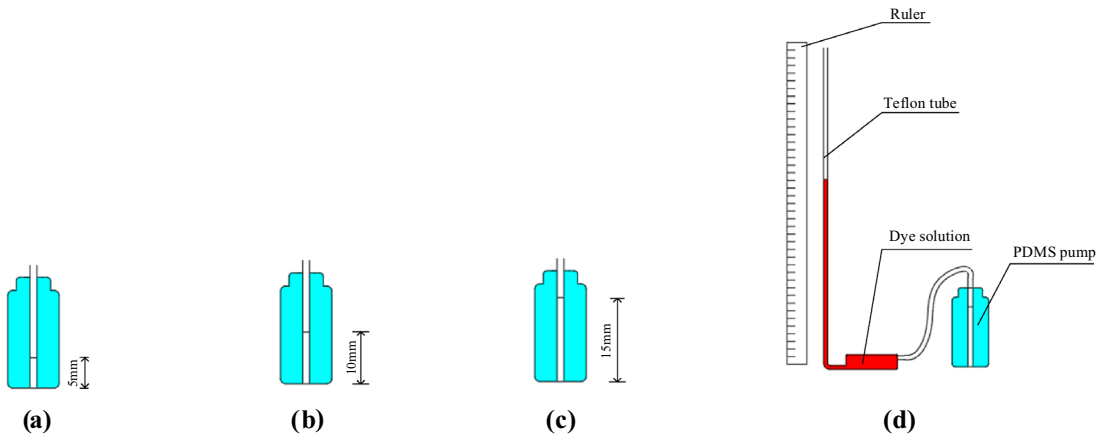

Fig. 2 Schematic drawing of the experimental setup for adjustment pumping capacity. **a** The Teflon tube is inserted into the center channel at 5 mm from the bottom. **b** The Teflon tube is inserted into the center channel at 10 mm from the bottom. **c** The Teflon tube is inserted into the center channel at 15 mm from the bottom. **d** The measurement for adjustment pumping capacity

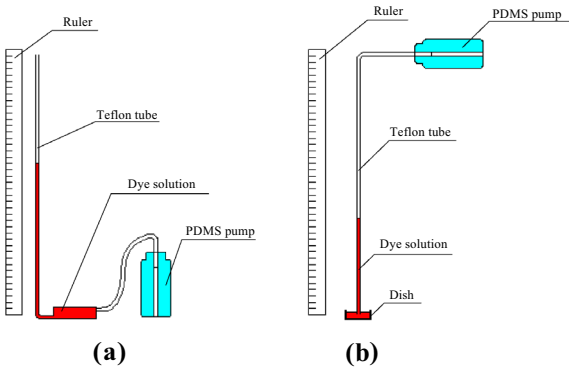

Fig. 3 Schematic drawing of the experimental setup for measuring the back pressure. **a** The measurement for positive pressure-driven PDMS pump. **b** The measurement for negative pressure-driven PDMS pump

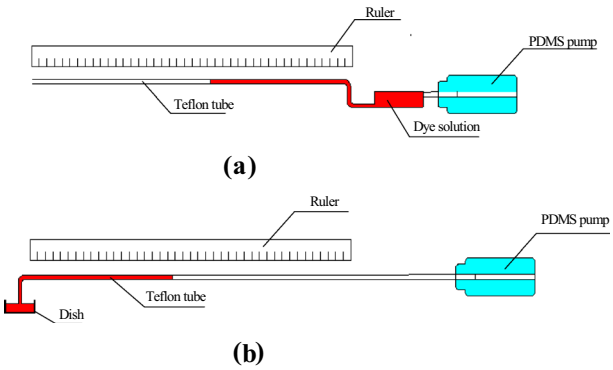

Fig. 4 Schematic drawing of the experimental setup for measuring the flow rate. **a** The measurement for positive pressure-driven PDMS pump. **b** The measurement for negative pressure-driven PDMS pump

rate of the fluid. A typical flow rate is less than 0.1 mm/s, which related to P_d is far less than P_s. Thus, the contribution of P_d is negligible in the calculation of P, and the pumping pressure (P) is simply calculated by the static fluid pressure (P_s).

The experimental setup for the back pressure measurement of positive pressure-driven PDMS pump is shown in Fig. 3a. The way of this experiment is similar to that of adjustment pumping capacity. The back pressure was evaluated by monitoring the elevation of the liquid column in the tube. A vertically positioned variable diameter Teflon tube with one end connected to the central channel of PDMS pump was used for measuring the back pressure. For all experiments, the PDMS pump was taken from the gasholder at 50 KPa for 24 h and the idle time was 2 min. Once the variable diameter part of the tube was filled with dye solution and inserted into the pump, the images were captured at an interval of 1 min using the CCD camera until the movement of the liquid stopped.

As shown in Fig. 3b, the measurement of back pressure for negative pressure-driven PDMS pump are similar to that for a positive one. And the back pressure was also calculated by monitoring the elevation of the liquid column in the tube. The negative pressure-driven PDMS pump was placed in a vacuum desiccator and degassed at 0 kPa for 24 h. Subsequently, the degassed PDMS pump was taken out from the vacuum chamber and tested the back pressure. Compare to the positive one, the Teflon tube's one end was inserted to the dish which was filled with dye solution and the other end was inserted into the negative-driven PDMS pump which was adhered to the wall.

The experimental setup for the flow rate measurements is shown in Fig. 4, which are similar to the measurement of back pressure. Figure 4a, b are respectively the measurements for the positive pressure-driven PDMS pump and the negative pressure-driven PDMS pump. The PDMS pump was assembled with a horizontally variable diameter tube and equipped with a CCD camera. When the measurement was begun, the images were captured at an interval of 30 s using the CCD camera until the movement of the liquid stopped. The flow rate was evaluated by monitoring the movement of the liquid column in the tube.

3.5 Sealing effect of PDMS pump

As shown in Fig. 1, the PDMS pump was sealed in a transfusion bottle, so several experiments on the sealing effect have been made. The sealing effect was measured by the test of the back pressure. A total of three groups of experiments were conducted immediately after being taken out of gasholder, 3 days later, and 5 days later. When the PDMS pumps were taken from the gasholder, screw the sealing cover at once and put it in the same environment as the PDMS pump which tested immediately. During the measurement, the positive-driven PDMS pumps which were taken from the gasholder at 50 KPa for 24 h, and then, one of the PDMS pumps was immediately tested and the rest was sealed for subsequent experiments. For all experiments, the idle time was 2 min and the Teflon tube was inserted into the center channel 15 mm from the bottom.

4 Results and discussion

4.1 Results of adjusting pumping capacity

As shown in Fig. 2, the pumping capacity of different adjustment modes are evaluated by monitoring the working time and height of elevation of the liquid column in the tube. Table 1 shows the experimental measurement results. Type (a) means the Teflon tube is inserted into

Table 1 Summary of pumping capacity for different kinds of adjustment modes

Type	Working time (min)	Rising height of liquid (cm)
(a)	82	37
(b)	103	64
(c)	120	83

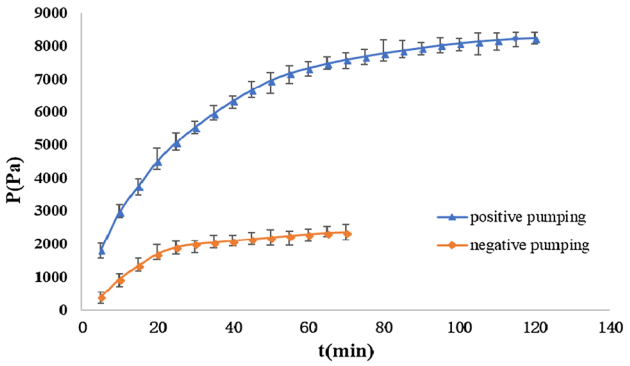

Fig. 5 Measurement results on the pumping pressure for positive/negative pumping

the center channel at 5 mm from the bottom. Type (b) means the Teflon tube is inserted into the center channel at 10 mm from the bottom. And type (c) means the Teflon tube is inserted into the center channel at 15 mm from the bottom. The pumping capacity of type (c) which tested immediately kept increasing for about 120 min. It can be seen from Table 1 that the rising height of liquid can reach 83 cm. However, the maximum rising height of liquid of type (a) is about 37 cm and there was no more increase after 37 min.

For the same PDMS pump, the time the liquid can be driven increases with the increase of the time of the PDMS pump aerated by the air compressor. Our group is studying the relationship between them. The PDMS pump aerated by the air compressor of experiments involved in this paper are 6 h, 12 h, 18 h and 24 h. The time the liquid can be driven by the PDMS pump are 47 min, 83 min, 109 min and 120 min.

4.2 Results of back pressure

As shown in Fig. 3, the back pressure was measured by monitoring the liquid level change in a Teflon tube when the PDMS pump is placed onto the elevator connected with the tube. Figure 5 shows the experimental measurement results of the back pressure after these positive pressure-driven PDMS pumps were taken out of gasholder. As a comparison, the negative-driven PDMS pumps were also tested immediately after being taken out of vacuum desiccator. In order to prove the reliability of the experimental results, these two kinds of PDMS pumps were tested three times respectively.

The back pressure of the positive pressure-driven PDMS pump which tested immediately kept increasing for about 120 min. It can be seen from Fig. 5 that the back pressure can reach about 8300 Pa. However, the maximum back pressure of negative pressure-driven PDMS pump is about 2300 Pa and there was not any more pressure increase after 70 min. Compared to the negative pumping, the back pressure of positive pressure-driven PDMS pump is about four times than it. The upper deviation and the lower deviation of the error bars in Fig. 5 respectively represent the maximum and minimum of experimental results. The points in the figure are the average values of the experiments. At 120 min, the back pressure of positive pumping can reach the maximum 8450 Pa and the minimum is 8000 Pa. The back pressure of negative pumping can reach the maximum 2600 Pa and the minimum at 70 min is 2000 Pa. Table 2 summaries the driving capacity for these two types of PDMS pump, which shows positive-driven PDMS pump has a strong driving capacity than the negative one.

4.3 Results of flow rate

Figure 6 shows the experimental measurement results of the flow rate which PDMS pumps are tested immediately after being taken out of gasholder or vacuum desiccator. To prove the reliability of the experimental results, these two kinds of PDMS pumps were tested three times, respectively. It can be seen in Fig. 6, the initial flow rate started with about 32.18 μL/min for positive pumping, and even 30 min later, there is still a relative high flow for the devices. While for the negative pumping, the initial flow rate started with about 16.48 μL/min and decreased to 0 in 30 min. The upper deviation and the lower deviation of the error bars

Table 2 Summary of driven capacity for different types of PDMS pump

Type	Unit-driven capacity (Pa/mm^3)	References
Negative pressure-driven PDMS pump	1.14	Li et al. (2012)
Negative pressure-driven PDMS pump	1.27	Measured in this paper
Positive pressure-driven PDMS pump	7.05	Measured in this paper

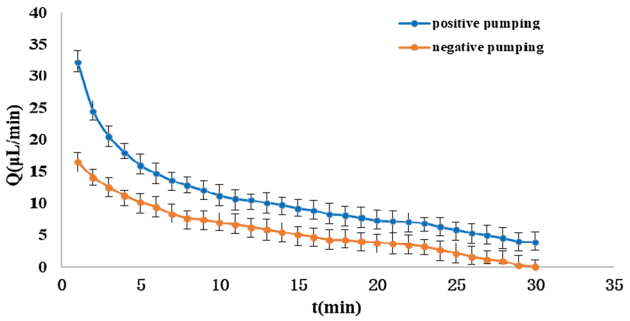

Fig. 6 Measurement results on the flow rate for positive/negative pumping

in Fig. 6, respectively represent the maximum and minimum of experimental results. The points in the figure are the average values of the experiments. The initial flow rate of positive pumping can reach the maximum 33.98 μL/min and the minimum is 30.56 μL/min. The initial flow rate of negative pumping can reach the maximum 17.92 μL/min and the minimum is 15.27 μL/min.

4.4 Results of sealing effect

Figure 7 shows the experimental measurement results of the sealing effect which PDMS pumps are tested immediately after being taken out of gasholder, 3 days later, and 5 days later. To prove the reliability of the experimental results, these three kinds of experiments were tested three times, respectively.

It can be seen in Fig. 7, the back pressure of the positive pressure-driven PDMS pump which was tested 3 days later kept increasing for about 60 min and the back pressure can reach 2650 Pa. Even after 6 days, it can still be reached 1120 Pa and kept working for 25 min. The upper deviation and the lower deviation of the error bars in Fig. 7, respectively, represent the maximum and minimum of experimental results. The points in the figure are the average values of the experiments. The measurement results of sealing effect

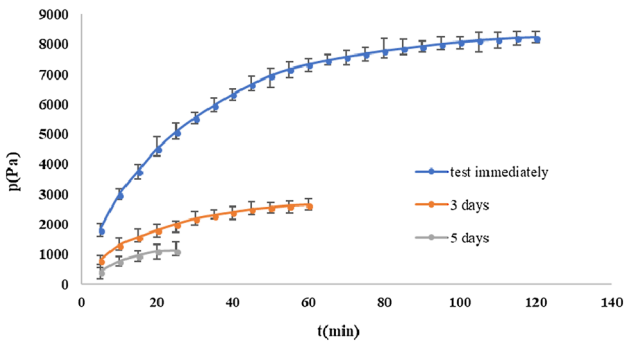

Fig. 7 Measurement results of sealing effect

which tested immediately can reach the maximum 8450 Pa and the minimum is 8000 Pa. The measurement results of sealing effect which tested after 3 days can reach the maximum 2870 Pa and the minimum is 2400 Pa. The measurement results of sealing effect which tested after 6 days can reach the maximum 1280 Pa and the minimum is 1050 Pa.

Possible causes of errors for back pressure (Fig. 5), flow rate (Fig. 6) and sealing effect (Fig. 7) are: (1) insertion position of the Teflon tube into the central channel position. Though the PDMS pump which the Teflon tube inserted into the center channel 15 mm from the bottom is used in this experiment, manual operation can still cause errors. (2) Idle time. In this experiment, the idle time was 2 min but the time difference between each step of preparation experiment within this 2 min will lead to errors. (3) Measurement of experimental results. The measurement of experimental results obtained by ruler, which will lead to measurement errors.

5 Application

5.1 Design and fabrication

To use easily, the aerated PDMS pump can be stored in a transfusion bottle (Fig. 8). In practical applications, a user only required to open the sealing cover, then use a Teflon tube to connect a PDMS pump and a microfluidic chip. This aerated PDMS pump not only provides convenience for user but also expands the application range. As shown in Fig. 8, we demonstrated the utility of this pumping method by applying it to a PDMS-based viscometer microfluidic device (30 mm × 15 mm × 5 mm).

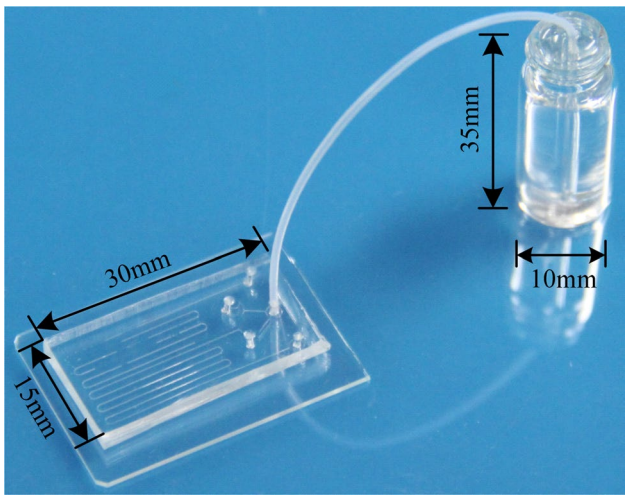

Fig. 8 A PDMS-based viscometer with positive pressure-driven PDMS pump

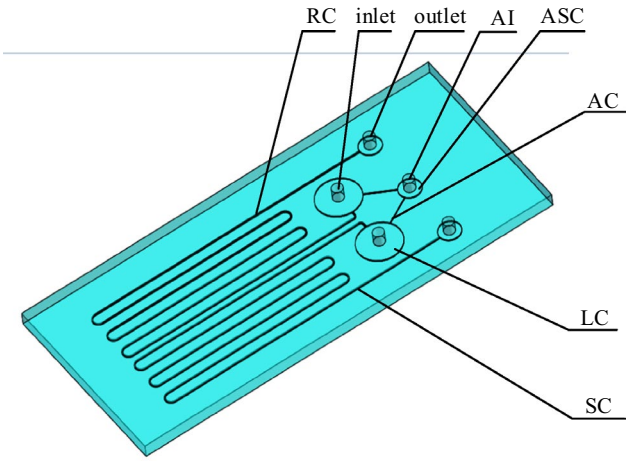

Fig. 9 Schematic overview of the PDMS-based viscometer microfluidic chip

As shown in Fig. 9, the PDMS viscometer microfluidic chip consisted of two liquid chambers (LC) ($r = 2000$ μm, $h = 100$ μm), two liquid inlets, an air inlet (AI), an air storage chamber (ASC) ($r = 1000$ μm, $h = 100$ μm), and two outlets. Here r and h are the radius and height of the chambers, respectively.

Microchannels between liquid chambers and air storage chamber are air channels (AC): ($L = 3000$ μm, $h = 100$ μm, $w = 100$ μm). Here, L, h and w are the length, height and width of the channels, respectively. Microchannels between liquid chambers and outlets are sample channel (SC) and reference channel (RC) ($L = 12$ cm, $h = 100$ μm, $w = 100$ μm).

The PDMS-based viscometer microfluidic chip was fabricated using standard soft lithography replica-molding techniques (Xia and Whitesides 1998). A mold was created using a negative photoresist, SU8-2050 (Micro-Chem Corp, Newton, MA, USA), which was spun onto a glass substrate using a spin coater (SC-1B, Beijing Jinshengweina Technology Co. Ltd, China). The resist was spread onto the glass substrate at 500 r/min for 10 s and then 1500 r/min for 20 s.

$$\frac{L^2_{\text{reference}}(t_2) - L^2_{\text{reference}}(t_1)}{t_2 - t_1} = \frac{\eta_{\text{sample}}}{\eta_{\text{reference}}} \frac{L^2_{\text{sample}}(t_2) - L^2_{\text{sample}}(t_1)}{t_2 - t_1} + 2d_h^2 \frac{P_{\text{c·reference}} - P_{\text{c·sample}}}{S\eta_{\text{reference}}} \tag{6}$$

The glass substrate was soft baked at 65 °C for 15 min and 95 °C for 120 min and then UV exposed for 6 min using a mask aligner (BGT-3B, Beijing Chuangweina Technology Co. Ltd, China). The glass substrate was then post baked for 15 min at 65 °C and 120 min at 95 °C, allowed to cool to room temperature, after developing and finally blown dry with nitrogen.

PDMS (Sylgard 184, Dow Corning) was prepared according to the instructions of the manufacturer, degassed in a vacuum chamber for 30 min, then poured onto the SU8 mold, and cured at hot plate for at 95 °C for 30 min. After that, PDMS was peeled off from the mold, five small holes with a diameter of about 0.6 mm were drilled on five chambers of the PDMS viscometer. Followed by oxygen plasma treatment for irreversible bonding between PDMS and glass slide at the top surface. Lastly, the chip was baked over a hot plate for 2 h at 95 °C to improve the bonding strength and stabilize the surface property of the devices.

5.2 Experimental

The PDMS-based viscometer was placed under a microscope (6XD-3, Shanghai Optical instrument, China) equipped with a CCD camera (Panasonic Super Dynamic II WV-CP460). A sample inlet was used to introduce the solution which need to measure its viscosity, and reference inlet was used to deionize water as a reference. A PDMS pump connected to the viscometer by a Teflon tube was used to drive the liquid flow in the viscometer. During the measurement, the CCD camera captured the images at an interval of 1 s for 50 s. The CCD images were analyzed by MATLAB to measure the distances of the running front of each stream from the inlets. The CCD images were opened with MATLAB, and the three-dimensional coordinate system was established based on PDMS-based viscometer dimensions. The starting and ending points were selected from the imdistline toolbox in MATLAB, and the length of each line could be calculated. The ratio of the viscosity of the solution to the viscosity of the reference fluid was determined from data analysis. In this experiment, absolute ethyl alcohol, isopropyl alcohol, and acetone were used to measure their viscosities. The experimental process of absolute ethyl alcohol as an example is shown in Fig. 10.

5.3 Analysis and results

From our previous analysis of the PDMS viscometer, we have (Han et al. 2007):

where $L(t)$ is the length of the fluid column inside the channel at time t with the subscripts reference and sample indicating the reference and sample fluids; η is the viscosity of the fluid; S is a constant related to channel geometry, and for a rectangular cross-section S is 32 (Perry and Green 2008); P_c is the pressure caused by capillary force; d_h is the hydraulic diameter of the channel.

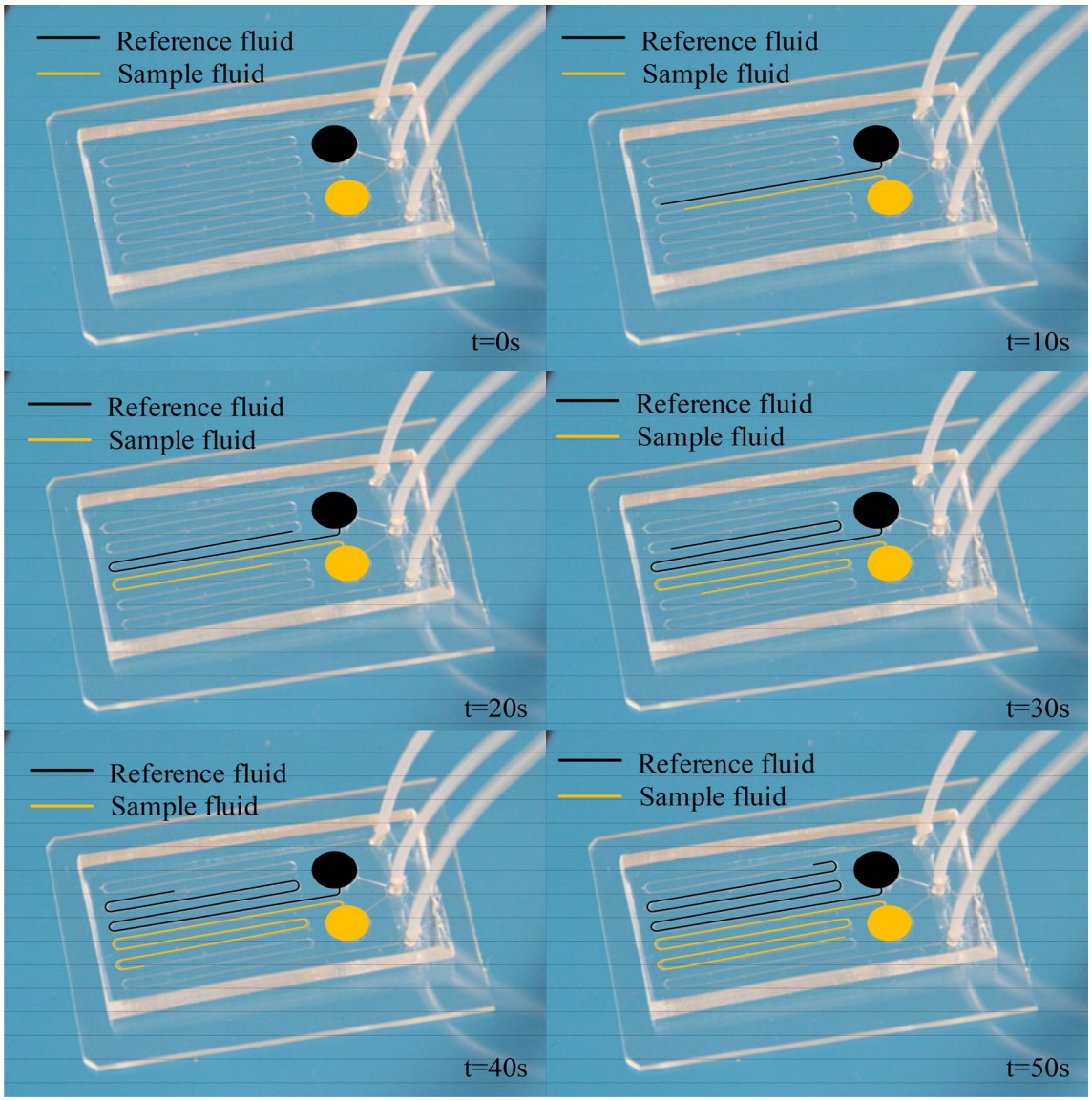

Fig. 10 Photos of a test run for absolute ethyl alcohol on the PDMS-based viscometer

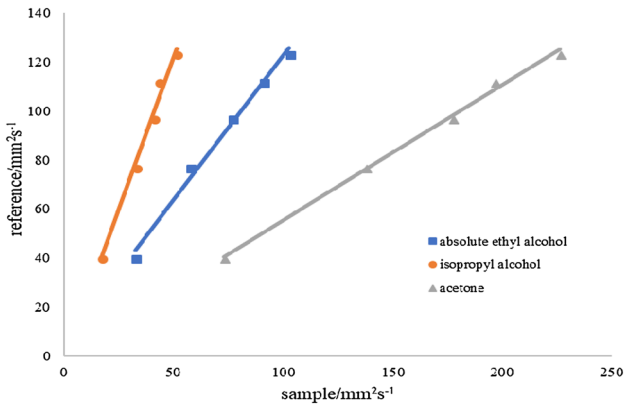

Fig. 11 The plot of sample versus reference of three liquids which measured by PDMS viscometer

Table 3 Viscosities of various fluids measured by PDMS viscometer at 20 °C

Sample	Normal viscosity (mPa s)	PDMS viscometer (mPa s)	Relative error (%)
Absolute ethyl alcohol	1.170	1.12	4.3
Isopropyl alcohol	2.37	2.29	3.3
Acetone	0.322	0.3	6.8

Assume that P_c is constant for both sample and reference fluids. Thus, $\eta_{sample}/\eta_{reference}$ was obtained by the slope value of the curve of $\left[L^2_{reference}(t_2) - L^2_{reference}(t_1)\right]/(t_2 - t_1)$ and $\left[L^2_{sample}(t_2) - L^2_{sample}(t_1)\right]/(t_2 - t_1)$ (Fig. 11). Each sam-

ple fluid was measured viscosity three times. And the coordinate in the Fig. 11 was the average value of experimental results. Then, the points were fitted into a straight line. The results after data analysis according to Eq. (6) is shown in Table 3. And compared to the normal viscosity, the viscosities of various fluids measured by PDMS viscometer obtained a good test accuracy for which the relative error range is about 5%.

This study only shows a case of positive pressure-driven PDMS pump in viscosity measurement. There are three general areas to be further investigated for positive pressure-driven PDMS pump: (1) mixing, (2) blood separation, and (3) droplet generation.

6 Conclusion

A positive pressure-driving technique-based PDMS pump has been developed. This paper presents a PDMS pump that utilizes the air release from the aerated PDMS to create a positive pressure for in microfluidic devices. Different from pumps in several existing microfluidic systems, the aerated PDMS pump can be easily removed and replaced, which increased system flexibility and reduced individual chip fabrication complexity due to its independence and versatility, meanwhile reducing the complexity and cost of microfluidic chips. In addition, the performance of the aerated PDMS pump were also investigated. These parameters include the adjustment of pumping capacity, sealing effect, pumping pressure and flow rate. The experimental results demonstrate that it is possible to flexibly build microfluidic system combination with an above-mentioned PDMS pump for achieving the desired function.

Acknowledgements This work was financially supported by National Natural Science Foundation of China (no. 51105011), Science and Technology Planning Project of Beijing Board of education, China (no. KM201210005015). I also want to thank Jane Zhang who has been giving me the strength.

References

Barker S, Rhoads E, Lindquist P et al (2016) Magnetic shape memory micro-pump for sub-microliter intracranial drug delivery in rats. J Med Devices 10(4):15948

Bourbaba E, Bouanini M, Benachaiba C (2016) Optimization of the performance of a biomedical micro-pump. Int J Multiphys 10(2):205–213

Das D (2016) Continuous microfluidic platforms for oil-in-water (O/W) emulsions for environmental monitoring applications. Dissertation, Nanyang Environment and Water Research Institute

Garg N, Vallejo D, Boyle D et al (2016) Integrated on-chip microfluidic immunoassay for rapid biomarker detection. Procedia Eng 159:53–57

George SC, Thomas S (2001) Transport phenomena through polymeric systems. Prog Polym Sci 26(6):985–1017

Goswami S, Klaus S, Benziger J (2008) Wetting and absorption of water drops on Nafion films. Langmuir ACS J Surf Colloids 24(16):8627–8633

Han Z, Tang X, Zheng B (2007) A PDMS viscometer for microliter Newtonian fluid. J Micromech Microeng 17(9):1828–1834

Hasegawa K, Matsumoto M, Hosokawa K et al (2015) Detection of methylated DNA on a power-free microfluidic chip with laminar flow-assisted dendritic amplification. Anal Sci 32(6):603–606

He X, Xu W, Lin N et al (2017) Dynamics modeling and vibration analysis of a piezoelectric diaphragm applied in valveless micropump. J Sound Vib 405:133–143

Hosokawa K, Sato K, Ichikawa N et al (2004) Power-free poly(dimethylsiloxane) microfluidic devices for gold nanoparticle-based DNA analysis. Lab Chip 4(3):181–185

Iverson BD, Garimella SV (2008) Recent advances in microscale pumping technologies: a review and evaluation. Microfluid Nanofluid 5(2):145–174

Li G, Luo Y, Chen Q et al (2012) A "place n play" modular pump for portable microfluidic applications. Biomicrofluidics 6(1):014118

Luo C, Zhu X, Yu T et al (2010) A fast cell loading and high-throughput microfluidic system for long-term cell culture in zero-flow environments. Biotechnol Bioeng 101(1):190–195

Manz A, Graber N, Widmer HM (1990) Miniaturized total chemical analysis systems: a novel concept for chemical sensing. Sens Actuators B Chem 1(1):244–248

Miller FP, Vandome AF et al (2010) Henry's law. Alphascript, Germany

Mojica WD, Oh KW, Lee H et al (2016) Microfluidics enables multiplex evaluation of the same cells for further studies. Cytopathology 27(4):277–283

Opekar F, Nesměrák K, Tůma P (2016) Electrokinetic injection of samples into a short electrophoretic capillary controlled by piezoelectric micropumps. Electrophoresis 37(4):595–600

Pandele AM, Comanici FE, Carp CA et al (2017) Synthesis and characterization of cellulose acetate-hydroxyapatite micro and nano composites membranes for water purification and biomedical applications. Vacuum 146:599–605

Perry RH, Green DW (2008) Perry's chemical engineers handbook. McGraw-Hill, New York

Sheikhlou M, Shabani R, Rezazadeh G (2015) Nonlinear analysis of electrostatically actuated diaphragm-type micropumps. Nonlinear Dyn 83(1–2):1–11

Skelley AM, Voldman J (2008) An active bubble trap and debubbler for microfluidic systems. Lab Chip 8(10):1733–1737

Smetana FO, Carley CT Jr (1966) An absolute high resolution calibrator for vacuum gauges. J Vacuum Sci Technol 3(2):49–53

Xia Y, Whitesides GM (1998) Soft lithography. Angew Chem Int Ed 37(5):550–575

Xu L, Lee H, Oh KW (2014) Syringe-assisted point-of-care micropumping utilizing the gas permeability of polydimethylsiloxane. Microfluid Nanofluid 17(4):745–750

Xu L, Lee H, Brasil Pinheiro MV et al (2015) Phaseguide-assisted blood separation microfluidic device for point-of-care applications. Biomicrofluidics 9(1):3163–3169